Advances in Water Resources 34 (2011) 375–382

Contents lists available at ScienceDirect

Advances in Water Resources

journal homepage: www.elsevier.com/locate/advwatres

Reduced complexity models for probabilistic forecasting of infiltration rates

Peng Wang, Daniel M. Tartakovsky *

Department of Mechanical and Aerospace Engineering, University of California, San Diego, 9500 Gilman Drive, Mail Code 0411, La Jolla, CA 92093-0411, USA

ARTICLE INFO

Article history:
Received 21 August 2010
Received in revised form 11 December 2010
Accepted 12 December 2010
Available online 21 December 2010

Keywords:
Uncertainty quantification
Stochastic
Risk assessment
Sorptivity
Vadose zone
Green–Ampt model

ABSTRACT

Soil heterogeneity and data sparsity combine to render estimates of infiltration rates uncertain. We develop reduced complexity models for the probabilistic forecasting of infiltration rates in heterogeneous soils during surface runoff and/or flooding events. These models yield closed-form semi-analytical expressions for the single- and multi-point infiltration-rate PDFs (probability density functions), which quantify predictive uncertainty stemming from uncertainty in soil properties. These solutions enable us to investigate the relative importance of uncertainty in various hydraulic parameters and the effects of their cross-correlation. At early times, the infiltration-rate PDFs computed with the reduced complexity models are in close agreement with their counterparts obtained from a full infiltration model based on the Richards equation. At all times, the reduced complexity models provide conservative estimates of predictive uncertainty.

1. Introduction

Reliable estimates of infiltration rates are notoriously elusive due to soil heterogeneity and the lack of sufficient site characterization. This ubiquitous parametric uncertainty requires model predictions to be accompanied by robust uncertainty quantification, which must accommodate realistic statistical descriptions of hydraulic parameters (saturated, K_s, and relative, K_r, hydraulic conductivities, and parameters in retention curves) in the flow equations. Probabilistic treatment of hydraulic parameters renders the corresponding flow equations stochastic, so that their solutions are given in terms of probability density functions (PDFs).

A standard practice in soil physics and subsurface hydrology is to compute the first two statistical moments of system states (e.g., pressure head ψ and water content θ) in lieu of full PDFs. Within this framework, ensemble means (first ensemble moments $\bar{\psi}$ and $\bar{\theta}$) serve as predictors of system behavior, and variances (second ensemble moments σ_ψ^2 and σ_θ^2) provide a measure of predictive uncertainty. Examples of such stochastic analyses of the Richards equation,

$$\frac{\partial\theta}{\partial t} = \nabla\cdot(K\nabla\psi) - \frac{\partial K}{\partial x_3}, \quad K = K_s K_r(\theta), \quad \theta = \theta(\psi), \tag{1}$$

include [41,18,15,27,32,29], among many others. Since these and numerous other studies aim to derive deterministic moment equations for means and (co)variances of system states, they are ill-suited for risk analyses and analyses of rare events, both of which require the knowledge of full PDFs [34,40,5]. Moreover, moment equations are applicable to either mildly heterogeneous or well-characterized soils. Unless the use of the Kirchhoff transformation is warranted [36,33,17], they also require linearization of the constitutive relations, $K_r = K_r(\theta)$ and $\theta = \theta(\psi)$, in the Richards equation (1). This limits the range of their applicability and introduces modeling errors that cannot be quantified a priori.

An alternative is to assume that a system state, e.g., pressure head $\psi(\mathbf{x},t)$ in (1), has a Gaussian PDF $p_\psi(\Psi;\mathbf{x},t)$ [1,2]. This approach provides a full probabilistic description of ψ required for risk assessment—it can be used, for example, to compute $\Pr[\psi(\mathbf{x},t)\leqslant\Psi] = \int_{\psi_{\min}}^{\Psi} p_\psi(\Psi';\mathbf{x},t)\mathrm{d}\Psi'$, the probability of uncertain (random) pressure head ψ at point $\mathbf{x}$ and time t not exceeding a given value Ψ—once its mean $\bar{\psi}(\mathbf{x},t)$ and variance $\sigma_\psi^2(\mathbf{x},t)$ are obtained from the corresponding deterministic moment equations [1,2]. Unfortunately, PDFs of $\psi(\mathbf{x},t)$ are in general non-Gaussian [35].

Monte Carlo simulations (MCS) provide another popular approach for solving the stochastic Richards equation (1), e.g., [13,7,8] among many others. In principle, MCS can be used to compute PDFs of dependent variables in the Richards equation. However, MCS of the transient three-dimensional Richards equation are typically computationally prohibitive, even when the goal is to compute the first two moments of $\theta(\mathbf{x},t)$ or $\psi(\mathbf{x},t)$. When used to compute PDFs of dependent variables, the reliability of MCS suffers from the arbitrariness of the bin-size selection associated with statistical analysis of simulation results. To the best of our knowledge, no PDF solutions of the Richards equation are reported in the literature.

* Corresponding author. Tel.: +1 1505 665 5757.
E-mail addresses: p7wang@ucsd.edu (P. Wang), dmt@ucsd.edu (D.M. Tartakovsky).

0309-1708/$ - see front matter © 2010 Elsevier Ltd. All rights reserved.
doi:10.1016/j.advwatres.2010.12.007

Given the practical impossibility of obtaining accurate PDF solutions of the stochastic Richards equation (1) in three spatial dimensions, we develop reduced complexity models to compute PDFs of the rate of infiltration into heterogeneous soils with uncertain hydraulic parameters. Construction of such models starts with the selection of a simplified statistical model for soil properties. In the present analysis, we will make use of the Dagan–Bresler statistical parameterization [9], which reduces the spatial dimensionality of random parameter fields. For example, saturated hydraulic conductivity $K_s(\mathbf{x})$—the sole source of uncertainty in [9]—is treated as a two-dimensional *random field*, $K_s(x_1,x_2)$, i.e., a soil is treated as a collection of vertical tubes each of which is characterized by a different *random variable* K_s.

The Dagan–Bresler parameterization [9] enables one to model three-dimensional infiltration with a collection of one-dimensional (in the x_3 direction) solutions of either the Richards equation (1) or its approximations, such as the Green–Ampt model [38] and the three-parameter infiltration equation of Parlange et al. [24]. Stochastic analyses of the Richards equation with the Dagan–Bresler parameterization can be found in [26,44]. Their counterparts based on the Green–Ampt equation were found to yield accurate predictions of infiltration into heterogeneous soils [6] and have been adopted in a number of subsequent investigations, e.g., [16,19,20,42]. These and other similar analyses aimed to derive effective (ensemble averaged) infiltration equations, and some of them quantified predictive uncertainty by computing variances of system states.

Our goal here is to provide a full probabilistic description of infiltration into heterogeneous soils with uncertain parameters (i.e., to compute PDFs of relevant dependent variables) by employing the reduced complexity models based on the Dagan–Bresler parameterization [9] and either the Green–Ampt [38] or the Parlange et al. [24] infiltration equations. From the outset, it is worthwhile emphasizing that the reliance on the Dagan–Bresler parameterization [9] formally limits our analysis to infiltration into top soils, and thus can be used to model surface response to rainfall events [19,20] and transport phenomena in top soil [42]. Yet it was also used to derive effective properties of the whole vadose zone [43,45]. Rubin and Or [26] provided an additional justification for the Dagan–Bresler parameterization by noting that "the determination of soil hydraulic properties through field methods. . .homogenize the properties vertically, thus eliminating the variability in the vertical direction in a practical sense."

The two alternative reduced complexity models are formulated in Section 3, which is preceded (Section 2) by a brief summary of experimental evidence used to select statistical properties of saturated hydraulic conductivity K_s and fitting parameters in the constitutive laws $K_r = K_r(\theta)$ and $\theta = \theta(\psi)$. Section 4 presents analytical closed-form expressions for the infiltration-rate PDFs that can be used as input for probabilistic forecasting of surface runoff and flooding. In Section 5, we investigate the temporal evolution of the infiltration-rate PDFs (Section 5.1), the relative importance of uncertainty in various hydraulic parameters (Section 5.2), and the effects of their cross-correlation (Section 5.3). A comparison of the PDFs obtained from the reduced complexity models with those computed by means of Monte Carlo simulations of the Richards equation (1) is presented in Section 5.4. Key findings of this analysis are summarized in Section 6.

2. Statistics of soil parameters

The vast majority of stochastic analyses reported in the literature deal with Gardner's model of the relative conductivity $K_r(\psi) = \exp(\alpha\psi)$, which facilitates theoretical developments but is seldom used in practice. The analysis below is applicable to an arbitrary choice of the relative hydraulic conductivity $K_r = K_r(\psi)$ and the retention curve $\theta = \theta(\psi)$, and does not require their linearization. To be concrete, we employ the van Genuchten model [38, Table 2.1],

$$K_r(\psi) = \frac{\left[1 - \psi_d^{mn}(1+\psi_d^n)^{-m}\right]^2}{(1+\psi_d^n)^{m/2}}, \quad \frac{\theta(\psi)-\theta_i}{\phi-\theta_i} = \frac{1}{(1+\psi_d^n)^m}, \tag{2}$$

where $\psi_d \equiv \alpha|\psi|$, $m = 1 - 1/n$, ϕ is the porosity, and θ_i is the irreducible water content.

Soil heterogeneity and data sparsity render the saturated hydraulic conductivity K_s and the fitting parameters in (2) uncertain. This uncertainty is quantified by treating such parameters as random fields, so that a soil parameter $\mathcal{A}(\mathbf{x},\omega)$ varies not only in the physical domain, $\mathbf{x} \in \mathcal{D}$, but also in the probability space $\omega \in \Omega$. A probability density function $p_{\mathcal{A}}$, which describes the latter variability, is inferred from measurements of $\mathcal{A}$ by invoking ergodicity. A compilation of field data used to justify the selection of PDFs $p_{\mathcal{A}}$ for each hydraulic parameter is presented below (see also [36,37]).

2.1. Saturated hydraulic conductivity, K_s

Despite some reservations [12,39], both the data reviewed in [36] and more recent data analyses [19,45] suggest that the traditional treatment of $K_s(\mathbf{x})$ as a log-normal random field is warranted.

2.2. Fitting parameters in (2)

The experimental evidence presented in [28,31,45] suggests that parameter $\alpha(\mathbf{x})$ can be treated as a log-normal field. It also shows that the coefficient of variation of α is much larger than that of the shape factor n, which supports the treatment of n as a deterministic constant. Likewise, since both porosity ϕ and irreducible water content θ_i typically exhibit lower spatial variations than either K_s or α, we treat them as deterministic constants. As will become apparent from the derivations in Section 4, our approach can readily account for uncertainty (randomness) in any of these parameters.

2.3. Cross-correlations between hydraulic parameters

Experimental evidence on cross-correlation between $K_s(\mathbf{x})$ and $\alpha(\mathbf{x})$ is inconclusive. Various data sets were used to conclude that $K_s(\mathbf{x})$ and $\alpha(\mathbf{x})$ are perfectly correlated [30], uncorrelated [21], or anti-correlated [43]. The approach we present below is capable of handling an arbitrary degree of cross-correlation between $K_s(\mathbf{x})$ and $\alpha(\mathbf{x})$. Finally, the data reviewed in [36], as well as more recent data reported in [45], suggest that the coefficient of variation (CV) of K_s is generally much larger than that of α, i.e., that the former is much more variable than the latter.

3. Reduced complexity models

Construction of our reduced complexity models consists of two steps. First, the Dagan–Bresler statistical parameterization is used in Section 3.1 to represent three-dimensional random fields $K_s(\mathbf{x})$ and $\alpha(\mathbf{x})$ as a collection of corresponding random variables K_s and α. Second, the Richards equation (1) is replaced with either the Green–Ampt [38] or the Parlange et al. [24] infiltration equations in Sections 3.2.1 and 3.2.2, respectively. To be specific, we consider infiltration under ponding, which is a prerequisite for overland flow [11]. Other infiltration regimes can be handled as well by modifying the Green–Ampt [38] and the Parlange et al. [24] infiltration equations accordingly. The accuracy of the infiltra-

tion-rate PDFs predicted with the reduced complexity models is assessed via comparison with its counterpart obtained from MCS of the Richards equation (1) in Section 5.4.

3.1. Statistical model for soil parameters

Following [9], we restrict our analysis to infiltration depths that do not exceed vertical correlation lengths λ_v of (random) soil parameters $\mathcal{A}(\mathbf{x},\omega)$. Then $\mathcal{A}=\mathcal{A}(x_1,x_2,\omega)$, so that a heterogeneous soil can be represented by a collection of one-dimensional (in the vertical direction x_3) homogeneous columns of length L_3, whose uncertain hydraulic properties are modeled as random variables (rather than random fields). The restriction $\lambda_v > L_3$ formally renders the Dagan–Bresler parameterization [9] suitable for heterogeneous top soils, and thus can be used to model surface response to rainfall events [20,19] and transport phenomena in top soil [42]. Yet it was also used to derive effective properties of the whole vadose zone [43,45].

Consider a three-dimensional flow domain $\Omega=\Omega_h\times[0,L_3]$, where Ω_h represents its horizontal extent. A discretization of Ω_h into N elements represents Ω by an assemblage of N columns of length L_3. This facilitates the complete description of a random field $\mathcal{A}(x_1,x_2,\omega)$—in the analysis below, $\mathcal{A}$ stands for K_s and α but can also include other hydraulic properties and the ponding pressure head ψ_0 at the soil surface $x_3=0$—with a joint probability function $p_{\mathcal{A}}(A_1,\dots,A_N)$. Probability density functions (PDFs) of hydraulic properties of the ith column are defined as marginal distributions,

$$p_{\mathcal{A}_i}(A_i)=\int p_{\mathcal{A}}(A_1,\dots,A_N)\mathrm{d}A_1,\dots,\mathrm{d}A_{i-1}\mathrm{d}A_{i+1},\dots,\mathrm{d}A_N. \tag{3}$$

Since statistical properties of soil parameters $\mathcal{A}$ are inferred from spatially distributed data by invoking ergodicity, the corresponding random fields (or their fluctuations obtained by data de-trending) must be stationary so that

$$p_{\mathcal{A}_i}=p_{\mathcal{A}}\quad\text{for}\quad i=1,\dots,N. \tag{4}$$

If soil parameters (e.g., K_s and α) are correlated, their statistical description requires the knowledge of a joint distribution. For multivariate Gaussian $Y_1=\ln K_s$ and $Y_2=\ln\alpha$, their joint PDF is given by

$$p_{Y_1,Y_2}(y_1,y_2)=\frac{1}{2\pi\sigma_{Y_1}\sigma_{Y_2}\sqrt{1-\rho^2}}\exp\left[-\frac{R}{2(1-\rho^2)}\right], \tag{5a}$$

where

$$R=\frac{(y_1-\overline{Y}_1)^2}{\sigma^2_{Y_1}}-2\rho\frac{y_1-\overline{Y}_1}{\sigma_{Y_1}}\frac{y_2-\overline{Y}_2}{\sigma_{Y_2}}+\frac{(y_2-\overline{Y}_2)^2}{\sigma^2_{Y_2}}; \tag{5b}$$

$\overline{Y}_i$ and σ_{Y_i} denote the mean and standard deviation of Y_i ($i=1,2$), respectively; and $-1\leqslant\rho\leqslant 1$ is the linear correlation coefficient between Y_1 and Y_2. The lack of correlation between Y_1 and Y_2 corresponds to setting $\rho=0$ in (5).

3.2. Simplified flow models

During infiltration into top soils, the Dagan–Bresler parameterization of soil heterogeneity can be supplemented with an assumption of vertical flow. The rationale for, and implications of, neglecting the horizontal component of flow velocity can be found in [9,26,16] and other studies reviewed in the introduction. This assumption obviates the need to solve a three-dimensional flow problem, replacing the latter with a collection of N one-dimensional flow problems to be solved in homogeneous soil columns with random but constant hydraulic parameters.

The second step in the construction of our reduced complexity models for probabilistic estimation of infiltration rates $i(t)$ replaces the Richards equation (1) with either the Green–Ampt [38] (Section 3.2.1) or Parlange et al. [24] (Section 3.2.2) infiltration equations. The accuracy of these reduced complexity models is investigated in Section 5.4 via comparison with Monte Carlo solutions of the two-dimensional Richards equation (1).

As mentioned above, we consider the Green–Ampt [38] and Parlange et al. [24] infiltration equations corresponding to ponding water of height ψ_0 at the soil surface $x_3=0$. Other infiltration scenarios can be handled in a similar manner by modifying these equations as discussed in the closing of this section.

3.2.1. Green–Ampt infiltration model

The Green–Ampt model of infiltration approximates an S-shaped wetting front with a sharp interface (infiltration depth) $x_f(t)$, which separates the uniformly "wet" ($\theta=\theta_{\mathrm{wet}}$) region behind the wetting front from a partially-saturated region with a uniform water content $\theta=\theta_\infty$ ahead of the front. To be specific, and without loss of generality, we set $\theta_{\mathrm{wet}}=\phi$ and $\theta_\infty=\theta_i$. If the x_3 coordinate is positive downward, Darcy's law defines macroscopic (Darcy's) flux q as (e.g., [38, Eq. (5-1)])

$$q=-K_s\frac{\psi_f-x_f-\psi_0}{x_f}. \tag{6}$$

Pressure head, ψ_f, at the infiltration depth $x_f(t)$ is often set to a "capillary drive",

$$\psi_f=-\int_{\psi_i}^{0}K_r(\psi)\,\mathrm{d}\psi, \tag{7}$$

where ψ_i is the pressure head corresponding to the water content θ_i. Theoretical derivations of this equation can be found in [22,4].

Mass conservation requires that the infiltration rate $i=q$, and that $i=\Delta\theta\mathrm{d}x_f/\mathrm{d}t$ where $\Delta\theta=\phi-\theta_i$. Combined with (6), this leads to an implicit expression for the infiltration depth $x_f(t)$,

$$x_f-(\psi_0-\psi_f)\ln\left(1+\frac{x_f}{\psi_0-\psi_f}\right)=\frac{K_s}{\Delta\theta}t. \tag{8}$$

which is applicable to time intervals during which the height of ponding water, ψ_0, remains approximately constant. Substituting $\psi_f(t)$ from (8) into (6) yields a Green–Ampt solution for the infiltration rate $i(t)$.

3.2.2. Parlange infiltration model

The Parlange et al. [24] infiltration model seeks to preserve a sigmoidal shape of infiltration fronts by postulating a functional form of the soil water diffusivity $D(\theta)\equiv K\mathrm{d}\psi/\mathrm{d}\theta$. Under ponded conditions, this equation takes the form [14],

$$I-K_it=(\psi_0+\psi_j)\frac{\Delta\theta K_s}{i-K_s}+\frac{S^2-2\psi_jK_s\Delta\theta}{2\Delta K}\ln\left(1+\frac{\Delta K}{i-K_s}\right), \tag{9}$$

where cumulative infiltration rate $I(t)$ is related to infiltration rate $i(t)$ by $i=\mathrm{d}I/\mathrm{d}t$, and $\Delta K\equiv K_s-K_i$ with $K_i\equiv K(\theta_i)$. Following [23,14], we approximate soil sorptivity S by

$$S^2=\int_{\theta_i}^{\phi}(\phi+\theta-2\theta_i)D(\theta)\mathrm{d}\theta. \tag{10}$$

Finally, the parameter ψ_j ($\psi_j<\psi$) represents a small pressure jump at saturation that is typically observed in soil–water characteristic curves. This soil parameter depends on the local pore structure, has limited range and effect on infiltration predictions, and remans "constant in time and independent of changing boundary conditions" [14]. Consequently, we treat ψ_j as a deterministic constant.

For constant ponding water heights ψ_0, solving (9) yields an implicit expression for the infiltration rate $i(t)$ [14],

$$t = \frac{K_s(\psi_0+\psi_j)\Delta\theta}{(i-K_s)\Delta K} - \frac{S^2-2\psi_j K_s\Delta\theta}{2\Delta K(i-K_i)} + \frac{S^2-2K_s\Delta\theta(\psi_0+2\psi_j)}{2(\Delta K)^2} \times \ln\left(1+\frac{\Delta K}{i-K_s}\right). \quad (11)$$

For brevity, we will call this expression the Haverkamp solution for infiltration under ponded conditions, after the first author of [14]. Note that (11) reduces to (8) if one sets the soil water diffusivity $D(\theta)$ to be a delta function [38, pp. 159–161].

Analytical solutions (8) and (11) correspond to ponded conditions with constant water heights ψ_0. Our reduced complexity models can handle other infiltration regimes by replacing (8) and (11) with their appropriate counterparts. For example, (11) can be replaced with the analytical solutions in [25,3] if infiltration is driven respectively by atmospheric pressure at the soil surface ($\psi_0 = 0$) or by temporally varying ponded water height $\psi_0(t)$. Likewise, infiltration under non-ponded conditions can be handled by replacing (8) with appropriately modified Green–Ampt solutions, many of which can be found in [38]. What is important is that a properly chosen reduced complexity model provides a mapping $i = i(K_s, \alpha)$.

4. PDF Solutions for Infiltration Rate

Let $G_i(i^\star; t) = P[i \leqslant i^\star]$ denote the cumulative distribution function of i at time t, i.e., the probability that the random infiltration rate i at time t does not exceed some value $i^\star$. Eqs. (8) and (11) define mappings $i = i(K_s, \alpha)$ for the two alternative reduced complexity models. These mappings enable one to compute the cumulative distribution function $G_i(i^\star; t)$ as

$$G_i(i^\star; t) = \int_0^\infty \int_0^{\alpha(i^\star, K_s)} p_{Y_1,Y_2}(K_s, \alpha)\frac{d\alpha\, dK_s}{\alpha K_s}. \quad (12)$$

The denominator in (12) reflects the transition from the joint Gaussian PDF for Y_1 and Y_2, to lognormal variables $K_s = \exp(Y_1)$ and $\alpha = \exp(Y_2)$. The PDF of the random (uncertain) infiltration rate, $p_i(i^\star; t)$, can be obtained as

$$p_i(i^\star; t) = \frac{dG_i(i^\star; t)}{di^\star}, \quad (13)$$

which yields

$$p_i(i^\star; t) = \int_0^\infty \frac{p_{Y_1,Y_2}[\alpha(i^\star, K_s), K_s]}{\alpha(i^\star, K_s)K_s}\frac{\partial\alpha(i^\star, K_s)}{\partial i^\star} dK_s. \quad (14)$$

While the analysis above deals with two uncertain parameters, K_s and α, it can be readily generalized to account for uncertainty in other soil parameters, such as the van Genuchten parameter n. If M soil properties are uncertain then their statistics are characterized by a joint PDF, $p_{Y_1,\ldots,Y_M}$; the cumulative distribution function G_i in (12) is defined in terms of an M dimensional integral; and the subsequent derivation is modified accordingly.

4.1. Green–Ampt infiltration model

Computation of the infiltration-rate PDF, p_i is facilitated by the change of the integration variable in (14),

$$p_i(i^\star; t) = \int_0^\infty \frac{p_{Y_1,Y_2}[K_s(i^\star, \alpha), \alpha]}{\alpha K_s(i^\star, \alpha)}\frac{\partial K_s(i^\star, \alpha)}{\partial i^\star} d\alpha. \quad (15)$$

Here p_{Y_1,Y_2} and $K_s(i^\star, \alpha)$ are given by (5) and (6), respectively; and the derivative $\partial K_s/\partial i^\star$ is obtained from (6) as the reciprocal of

$$\frac{\partial i^\star}{\partial K_s} = 1 + \frac{\psi_0-\psi_f}{x_f}\left(1 - \frac{K_s t}{\Delta\theta}\frac{x_f-\psi_f+\psi_0}{x_f^2}\right). \quad (16)$$

4.2. Parlange infiltration model

For the van Genuchten constitutive relation (2), the soil sorptivity S in (10) takes the form

$$S^2 = \frac{K_s\Delta\theta}{\alpha}(1-m)A(m), \quad (17a)$$

where m is the van Genuchten model shape parameter, $A(m)$ is given by

$$A = \frac{\Gamma(1-m)\Gamma(3m/2-1)}{\Gamma(m/2)} - \frac{4}{3m-2} + \frac{\Gamma(m+1)\Gamma(3m/2-1)}{\Gamma(5m/2)} + \frac{\Gamma(1-m)\Gamma(5m/2-1)}{\Gamma(3m/2)} - \frac{4}{5m-2} + \frac{\Gamma(m+1)\Gamma(5m/2-1)}{\Gamma(7m/2)} \quad (17b)$$

and $\Gamma(\cdot)$ is the complete Gamma function. For the sake of simplicity, and without loss of generality, we assume that the soil ahead of the wetting front is "dry", and set $\psi_i = -\infty$. (Other values of ψ_i can be handled as well by following the procedure outlined below.) Then $K_i = 0$ and substituting (17) into (11) yields an explicit relation between the three random variables $\alpha = \alpha(i, K_s)$,

$$\alpha(i, K_s) = A\left[K_s - i\ln\left(\frac{i}{i-K_s}\right)\right]\frac{i-K_s}{2B(i, K_s)}, \quad (18a)$$

where

$$B(i, K_s) = (\psi_0+\psi_{str})iK_s - (\psi_0+2\psi_{str})i(i-K_s)\ln\left(\frac{i}{i-K_s}\right) + K_s(i-K_s)\left(\psi_{str} - \frac{it}{\Delta\theta}\right). \quad (18b)$$

Substituting (18) into (14) gives the infiltration-rate PDF,

$$p_i(i^\star; t) = \frac{A}{2}\int_0^\infty \frac{K_s p_{Y_1,Y_2}[\alpha(i^\star, K_s), K_s]}{\alpha(i^\star, K_s)B(i^\star, K_s)^2}\left\{\frac{K_s-i^\star}{\Delta\theta}K_s t - (\psi_0+\psi_{str})\left[(2i^\star-K_s)\ln\left(\frac{i^\star}{i^\star-K_s}\right) - 2K_s\right]\right\} dK_s. \quad (19)$$

4.3. Multi-point PDFs

As discussed in Section 3.1, a complete description of the random infiltration rate $i(\mathbf{x}, t)$ in the domain discretized into N elements requires the knowledge of an N-point PDF, $p_{\mathbf{i}}(i_1^\star, \ldots, i_N^\star; t)$, where $i_k^\star$ is a deterministic value (outcome) of the random infiltration rate i at the kth column ($k = 1, \ldots, N$). The reduced complexity models presented in Section 3 allow one to compute such multi-point PDFs.

Consider a two-point PDF, $p_{\mathbf{i}}^{(2)}(i_1^\star, i_2^\star; t)$, which describes a joint distribution of infiltration rates $i(\mathbf{x}^k, t)$ ($k = 1,2$) at points $\mathbf{x}^1 = (x_1^1, x_2^1)^T$ and $\mathbf{x}^2 = (x_1^2, x_2^2)^T$. Let $Y_{1,k} = \ln K_s(\mathbf{x}^k)$ and $Y_{2,k} = \ln\alpha(\mathbf{x}^k)$, with the joint two-point PDF $p_{Y_{1,1},Y_{2,1},Y_{1,2},Y_{2,2}}^{(2)}(Y_{1,1}^\star, Y_{2,1}^\star; Y_{1,2}^\star, Y_{2,2}^\star)$. Recalling that (6)–(8) and (11) define the two alternative mappings $i = i(K_s, \alpha)$, we compute, in analogy with (12), the two-point cumulative distribution function $G_{\mathbf{i}}^{(2)}(i_1^\star, i_2^\star; t)$ as

$$G_{\mathbf{i}}^{(2)}(i_1^\star, i_2^\star; t) = \int_0^\infty\int_0^\infty\int_0^{\alpha_1(i_1^\star, K_{s1})}\int_0^{\alpha_2(i_2^\star, K_{s2})} p_{Y_1,Y_2}^{(2)}(K_{s1}, \alpha_1; K_{s2}, \alpha_2) \times \frac{d\alpha_1 dK_{s1} d\alpha_2 dK_{s2}}{\alpha_1 K_{s1}\alpha_2 K_{s2}}. \quad (20)$$

The two-point PDF of the random (uncertain) infiltration rate, $p_{\mathbf{i}}^{(2)}(i_1^\star, i_2^\star; t)$, is obtained as

$$p_{\mathbf{i}}^{(2)}(i_1^\star, i_2^\star; t) = \frac{\partial^2 G_{\mathbf{i}}^{(2)}}{\partial i_1^\star \partial i_2^\star}. \quad (21)$$

N-point PDFs, $p_{\mathbf{i}}^{(N)}$ with $N > 2$, can be computed in a similar manner.

Table 1
Hydraulic properties of the Bet–Dagan soil [28, Table 3].

	$\ln K_s$(cm/min)	$\ln\alpha$ (cm^{-1})	ϕ	θ_i	ψ_0 (cm)	ψ_j (cm)	van Genuchten n
Mean	−3.58	−3.01	0.42	0.13	1	2	1.81
Variance	0.89	0.63	–	–	–	–	–

N-point PDFs can be used both to predict (cross-) correlations of infiltration rates at multiple locations and to assimilate infiltration data via a straightforward Bayesian updating. We leave the latter aspect for future investigation.

5. Results and discussion

The impact of various aspects of parametric uncertainty on the uncertainty in predictions of infiltration rate $i(t)$ obtained with the Green–Ampt model was investigated in [37]. Here we carry out a similar analysis for the infiltration-rate PDF predicted with the Parlange model (Haverkamp solution). Specifically, we investigate temporal evolution of the infiltration-rate PDF (Section 5.1), the relative importance of uncertainty in K_s and α (Section 5.2) and the effects of cross-correlation between them (Section 5.3). Finally, we compare the infiltration-rate PDFs computed with the two reduced complexity models and with MCS of the Richards equation (Section 5.4).

To be concrete, we use the Bet–Dagan soil properties [28] reported in Table 1. Unless explicitly noted otherwise, the simulations reported below correspond to the ponding water height $\psi_0 = 1$ cm, pressure jump $\psi_j = 2$ cm, and the cross-correlation coefficient $\rho = 0$.

5.1. Temporal evolution of infiltration rate PDFs

Fig. 1 presents three snapshots of the temporal evolution of the infiltration-rate PDF, $p_i(i;t)$, at times $t = 5$, 50 and 100 min. Uncertainty associated with predictions of the infiltration rate under ponded conditions (i.e., the width of p_i) decreases with time. This is because, as time increases, top soil gradually saturates and the infiltration rate $i(t)$ approaches an (uncertain) value of the saturated hydraulic conductivity K_s in accordance with (11), i.e., $p_i(i^\star;t) \to p_K(K_s^\star)$ as $t \to \infty$.

It must be noted that at large times, the infiltration depth exceeds the vertical correlation lengths of K_s and α, which violates the conditions of validity of the reduced complexity models. Therefore, our analysis is formally limited to early infiltration times and ought to be used to compute the infiltration-rate PDFs that are necessary for probabilistic forecasting of surface runoff and flooding where uncertainty in infiltration rate predictions is highest (Fig. 1). Unless otherwise noted the subsequent figures correspond to $t = 5$ min.

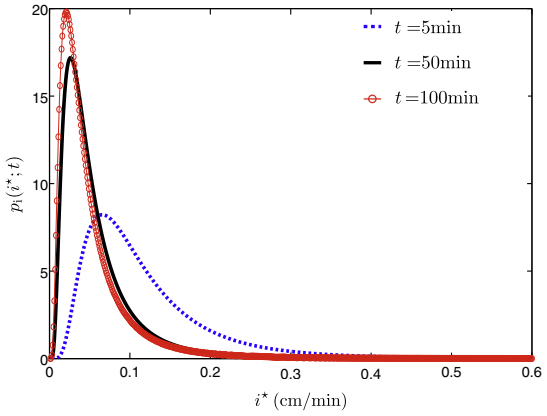

Fig. 1. Temporal evolution of the infiltration-rate PDF $p_i(i^\star;t)$ given by (19).

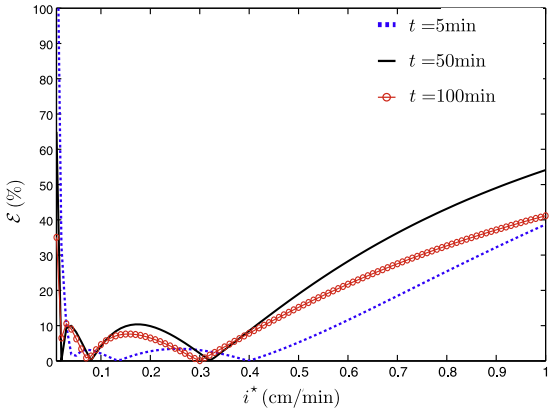

Fig. 2. Relative error, $\mathcal{E} \equiv 100\% \times |p_i - p_{\ln}|/p_i$, introduced by approximating the infiltration-rate PDF $p_i(i^\star;t)$ with its lognormal counterpart $p_{\ln}(i^\star;t)$.

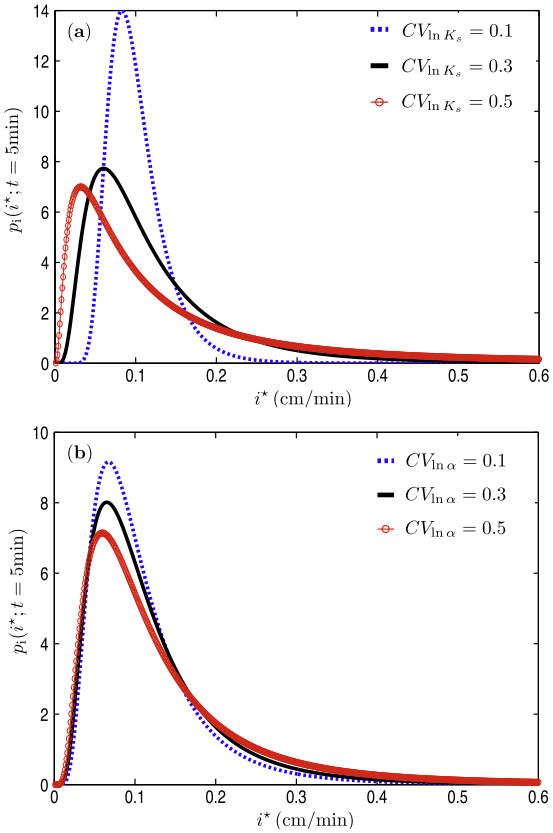

Fig. 3. The infiltration-rate PDF $p_i(i^\star;t = 5$ min) for different levels of uncertainty in (a) saturated hydraulic conductivity K_s and (b) the van Genuchten parameter α.

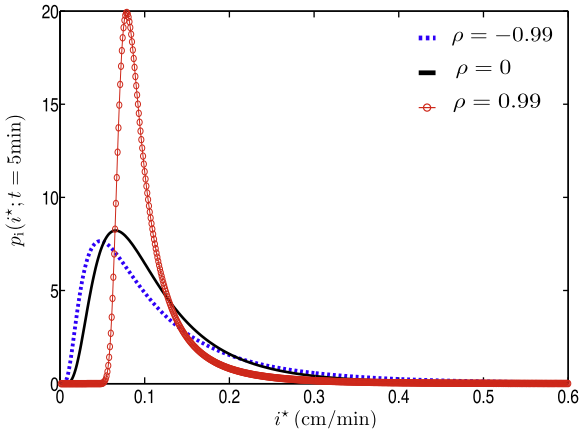

Fig. 4. The infiltration-rate PDF $p_i(i^\star; t = 5$ min) for three degrees of correlation ρ between hydraulic parameters K_s and α.

The infiltration-rate PDFs exhibit long tails that superficially resemble those of lognormal distributions. To test whether a lognormal distribution $p_{\ln}(i^\star; t)$ can be used to approximate $p_i(i^\star; t)$ in (19), we compute a relative error $\mathcal{E} \equiv 100\% \times |p_i - p_{\ln}|/p_i$. Both distributions have the same mean and variance. Fig. 2 reveals a significant discrepancy between the tails of the two distributions (probabilities of rare events).

5.2. Effects of parametric uncertainty

While the proposed approach can handle uncertainty in any number of hydraulic parameters, we focus on K_s and α for the reasons discussed above. In this section, we investigate the relative importance of these two sources of parametric uncertainty. Uncertainty in both $\ln K_s$ and $\ln\alpha$ is encapsulated in their respective coefficients of variation, $CV_{\ln K_s} \equiv \sigma_{Y_1}/\overline{Y}_1$ and $CV_{\ln\alpha} \equiv \sigma_{Y_2}/\overline{Y}_2$. Fig. 3 demonstrates their effects on predictive uncertainty (PDF of i at $t = 5$ min). The curves represent $p_i(i^\star;\ t = 5$ min) for the CV of one parameter set to 0.1, 0.3, 0.5 and the other parameter fixed at its value in Table 1. One can see that uncertainty in K_s has a more pronounced effect on the predictive uncertainty than uncertainty in α does. This finding is in accordance with previous observations [8–10,37].

5.3. Effects of cross-correlation

The data reviewed in Section 2 suggest that the presence, absence, or strength of cross-correlation between saturated hydraulic conductivity K_s and the van Genuchten parameter α is site-specific rather than universal. Our reduced complexity models allow one to investigate the role of this cross-correlation on predictive uncertainty in infiltration rates $i(t)$. Fig. 4 presents the infiltration-rate PDFs $p_i(i^\star; t)$ corresponding to K_s and α that are anti-correlated ($\rho = -0.99$), uncorrelated ($\rho = 0.0$) and perfectly correlated ($\rho = 0.99$). The comparison of the three curves reveals that the perfect correlation between K_s and α significantly reduces the predictive uncertainty.

5.4. Comparison with Richards' equation

To validate our reduced complexity models, we compare their PDF solutions with that obtained by Monte Carlo simulations (MCS) of the two-dimensional stochastic Richards equation (1). In these MCS, we used the geostatistical software library SGEMS to generate $N = 2000$ realizations of mutually-uncorrelated random

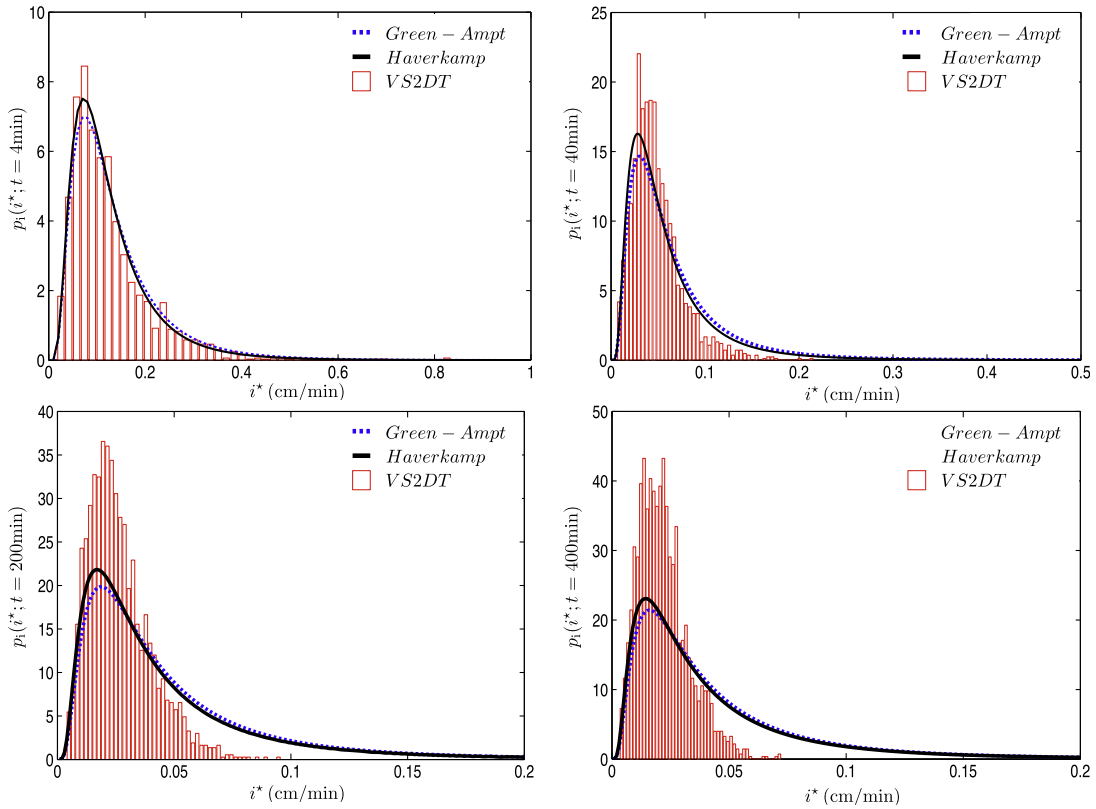

Fig. 5. Temporal snapshots of the infiltration-rate PDFs computed with the two reduced complexity models (Green–Ampt and Haverkamp) and Monte Carlo simulations of the Richards equation (VS2DT). Ratios of the horizontal and vertical correlation lengths are $\lambda_v/\lambda_h = 18.75$ and 30.0 for $\ln K_s$ and $\ln\alpha$, respectively.

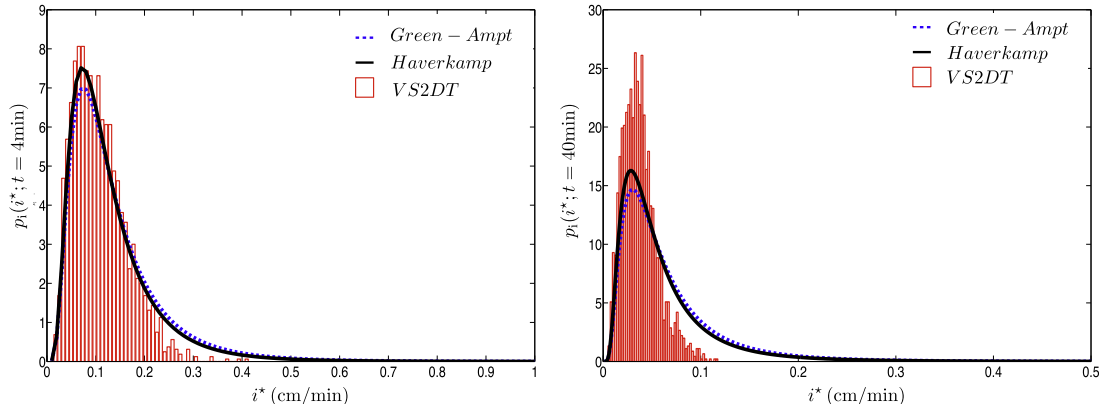

Fig. 6. Temporal snapshots of the infiltration-rate PDFs computed with the two reduced complexity models (Green–Ampt and Haverkamp) and Monte Carlo simulations of the Richards equation (VS2DT). Ratios of the horizontal and vertical correlation lengths are $\lambda_v/\lambda_h = 4.0$ and 2.5 for $\ln K_s$ and $\ln\alpha$, respectively.

fields $K_s(\mathbf{x})$ and $\alpha(\mathbf{x})$ in a two-dimensional (15,000 × 200 cm) domain discretized into 2500 nodes. For both parameters, we used an anisotropic exponential correlation function, with horizontal and vertical correlation lengths λ_h and λ_v, respectively. For each realization of $K_s(\mathbf{x})$ and $\alpha(\mathbf{x})$, the Richards equation was solved with the USGS code VS2DT, and the infiltration rate $i(t)$ was determined at a surface midpoint. The results were used to compute the infiltration-rate PDF as $p_i(i^\star; t) = (N\Delta_{bin})^{-1}\sum_{n=1}^{N} I(i_n \in \Delta_{bin}^{i^\star}; t)$, where Δ_{bin} is a (uniform) bin size, $\Delta_{bin}^{i^\star}$ is the bin containing $i^\star$, and I is the indicator function.

The Dagan–Bresler statistical parameterization, which forms the foundation of our reduced complexity models, requires that $\lambda_v \ll \lambda_h$. This requirement was tested by setting $\lambda_v/\lambda_h = 18.75$ and 30.0 for the random fields $\ln K_s$ and $\ln\alpha$, respectively. Fig. 5 compares the infiltration-rate PDF computed via MCS of the Richards equation with those determined analytically from both the Green–Ampt (Section 4.1) and Haverkamp (Section 4.2) solutions. These analytical solutions used the same random values of K_s and α at the surface midpoint as those used in the MCS. The PDFs computed with the two reduced complexity models are similar, with the Haverkamp solution having a slight edge. Both agree with the PDF resulting from the Richards equation at early times, but this agreement deteriorates with time. This is to be expected, since the conditions of validity of our reduced complexity models are violated as time becomes large enough for the wetting front to travel distances larger than the vertical correlation lengths of K_s and α.

Fig. 6 provides a similar comparison for smaller ratios of λ_v/λ_h. The ratios $\lambda_v/\lambda_h = 4.0$ and 2.5 for $\ln K_s$ and $\ln\alpha$ correspond to those observed in the Bet–Dagan soil [28]. The reduced complexity models perform well at early times ($t = 4$ min) but their accuracy deteriorates faster (by $t = 40$ min), reflecting the increased importance of the lateral flow. At all times and for arbitrary correlation-length ratios, the reduced complexity models provide conservative estimates of predictive uncertainty.

6. Conclusions

We presented two reduced complexity models for the probabilistic forecasting of infiltration rates in heterogeneous soils during surface runoff and/or flooding events. The models are based alternatively on the Green–Ampt or Parlange models of infiltration under ponded conditions, both employing the Dagan–Bresler statistical parameterization. These models yield closed-form semi-analytical expressions for the infiltration-rate PDFs (probability density functions), which quantify predictive uncertainty stemming from uncertainty in a soil's hydraulic parameters. Our analysis leads to the following major conclusions.

(1) The infiltration-rate PDFs developed in this analysis allow one to evaluate probabilities of rare events, i.e., to estimate the probability of the infiltration rate exceeding a given value.
(2) Predictive uncertainty (the infiltration-rate PDF) is significantly more sensitive to the coefficient of variation of saturated hydraulic conductivity K_s than to that of the fitting parameters in the van Genuchten hydraulic function.
(3) The degree of cross-correlation between hydraulic parameters K_s and α has great influence on predictive uncertainty.
(4) The PDFs computed with the two reduced complexity models are similar, with the Parlange model having a slight edge.
(5) At early times the PDFs obtained from both models agree with their counterpart resulting from the Richards equation, but this agreement deteriorates with time. The larger the ratio of horizontal and vertical correlation lengths of soil properties, the longer the reduced complexity models remain valid.
(6) At all times and for arbitrary correlation-length ratios, the reduced complexity models provide conservative estimates of predictive uncertainty.
(7) Nonlinear dependence of the infiltration rate on soil hydraulic parameters implies that the infiltration-rate PDF is in general not lognormal even if PDFs of the soil parameters are. Hence the nonlinear PDF mapping (14) should be used.

Reliance on the reduced complexity models of infiltration into heterogeneous soils with uncertain hydraulic parameters offers a number of advantages. Not only it allows one to compute single-point PDFs of the infiltration rate, it does so exactly, without introducing linearization errors that plague most stochastic analyses of the Richards equation. The reduced complexity models are capable of quantifying uncertainty in any number of hydraulic parameters and can be used with arbitrary constitutive laws (relative conductivity functions and retention curves). Finally, they make it possible to compute multi-point PDFs of infiltration rate. The latter can be used both to predict (cross-)correlations of infiltration rates at multiple locations and to assimilate infiltration data via a straightforward Bayesian updating.

The infiltration-rate PDFs presented here correspond to ponded conditions with constant water heights ψ_0. Other infiltration regimes can be handled in a similar manner by replacing (8) and (11) with their appropriate counterparts. For example, (11) can be replaced with the analytical solutions in [25,3] if infiltration is driven respectively by atmospheric pressure at the soil surface ($\psi_0 = 0$) or by temporally varying ponded water height $\psi_0(t)$. Likewise, infiltration under non-ponded conditions can be handled by

replacing (8) with appropriately modified Green–Ampt solutions, many of which can be found in [38]. What is important is that a properly chosen reduced complexity model provides a mapping $i = i(K_s, \alpha)$.

References

[1] Amir O, Neuman SP. Gaussian closure of one-dimensional unsaturated flow in randomly heterogeneous soils. Transp Porous Media 2001;44(2):355–83.
[2] Amir O, Neuman SP. Gaussian closure of transient unsaturated flow in random soils. Transp Porous Media 2004;54(1):55–77.
[3] Barry DA, Parlange J-Y, Haverkamp R, Ross PJ. Infiltration under ponded conditions: 4. An explicit predictive infiltration formula. Soil Sci 1995;160(1):8–17.
[4] Barry DA, Parlange J-Y, Sander GC, Sivaplan M. A class of exact solutions for Richards' equation. J Hydrol 1993;142(1–4):29–46.
[5] Bolster D, Barahona M, Dentz M, Fernandez-Garcia D, Sanchez-Vila X, Trinchero P, et al. Probabilistic risk analysis of groundwater remediation strategies. Water Resour Res 2009;45:W06413. doi:10.1029/2008WR007551.
[6] Bresler E, Dagan G. Unsaturated flow in spatially variable fields. 2. Application of water flow models to various fields. Water Resour Res 1983;19(2):421–8.
[7] Cassiani G, Binley A. Modeling unsaturated flow in a layered formation under quasi-steady state conditions using geophysical data constraints. Adv Water Resour 2005;28(5):467–77.
[8] Coppola A, Basile A, Comegna A, Lamaddalena N. Monte Carlo analysis of field water flow comparing uni- and bimodal effective hydraulic parameters for structured soil. J Contam Hydrol 2009;104(1–4):153–65.
[9] Dagan G, Bresler E. Unsaturated flow in spatially variable fields. 1. Derivation of models of infiltration and redistribution. Water Resour Res 1983;19(2):413–20.
[10] Foussereau X, Graham W, Rao P. Stochastic analysis of transient flow in unsaturated heterogeneous soils. Water Resour Res 2000;36(4):891–910.
[11] Freeze RA. A stochastic-conceptual analysis of rainfall-runoff processes on a hillslope. Water Resour Res 1980;16(2):391–408.
[12] Gómez-Hernández JJ, Wen X. To be or not to be multi-Gaussian? A reflection on stochastic hydrogeology. Adv Water Resour 1998;21(1):47–61.
[13] Harter T, Yeh TJ. Flow in unsaturated random porous media, nonlinear numerical analysis and comparison to analytical stochastic models. Adv Water Resour 1998;22(3):257–72.
[14] Haverkamp R, Parlange J-Y, Starr JL, Schmitz G, Fuentes C. Infiltration under ponded conditions: 3. A predictive equation based on physical parameters. Soil Sci 1990;149(5):292–300.
[15] Hu X, Cushman J. Nonequilibrium statistical mechanical derivation of a nonlocal Darcy's law for unsaturated/saturated flow. Stoch Hydrol Hydraul 1994;8(2):109–16.
[16] Indelman P, Touber-Yasur I, Yaron B, Dagan G. Stochastic analysis of water flow and pesticides transport in a field experiment. J Contam Hydrol 1998;32(1-2):77–97.
[17] Lu Z, Neuman SP, Guadagnini A, Tartakovsky DM. Conditional moment analysis of steady state unsaturated flow in bounded, randomly heterogeneous soils. Water Resour Res 2002;38(4). doi:10.1029/2001WR000278.
[18] Mantoglou A, Gelhar LW. Stochastic modeling of large-scale transient unsaturated flow system. Water Resour Res 1987;23(1):37–46.
[19] Meng H, Green TR, Salas JD, Ahuja LR. Development and testing of a terrain-based hydrologic model for spatial Hortonian infiltration and runoff/on. Environ Model Soft 2008;23(6):794–812.
[20] Morbidelli R, Corradini C, Govindaraju RS. A simplified model for estimating field-scale surface runoff hydrographs. Hydrol Process 2007;21(13):1772–9.
[21] Mualem Y. A new model for predicting the hydraulic conductivity of unsaturated porous media. Water Resour Res 1976;12(3):513–22.
[22] Neuman SP. Wetting front pressure head in the infiltration model of Green and Ampt. Water Resour Res 1976;12(3):564–6.
[23] Parlange J-Y. On solving the flow equation in unsaturated soils by optimization: horizontal infiltration. Soil Sci Soc Am Proc 1975;39:415–8.
[24] Parlange J-Y, Lisel I, Braddock RD, Smith RE. The three-parameter infiltration equation. Soil Sci 1982;133(6):337–41.
[25] Parlange J-Y, Haverkamp JTR. Infiltration under ponded conditions: 1. Optimal analytical solution and comparison with experimental observations. Soil Sci 1985;139:305–11.
[26] Rubin Y, Or D. Stochastic modeling of unsaturated flow in heterogeneous soils with water uptake by plant roots: the parallel columns model. Water Resour Res 1993;29(3):619–31.
[27] Russo D. Stochastic analysis of the velocity covariance and the displacement covariance tensors in partially saturated heterogeneous anisotropic porous formations. Water Resour Res 1995;31(7):1647–58.
[28] Russo D, Bouton M. Statistical analysis of spatial variability in unsaturated flow parameters. Water Resour Res 1992;28(7):1911–25.
[29] Russo D, Fiori A. Stochastic analysis of transport in a combined heterogeneous vadose zone–groundwater flow system. Water Resour Res 2009;45. doi:10.1029/2008WR007157.
[30] Russo D, Russo I, Laufer A. On the spatial variability of parameters of the unsaturated hydraulic conductivity. Water Resour Res 1997;33(5):947–56.
[31] Saito H, Seki K, Simunek J. An alternative deterministic method for the spatial interpolation of water retention parameters. Hydrol Earth Syst Sci 2009;13:453–65.
[32] Severino G, Santini A. On the effective hydraulic conductivity in mean vertical unsaturated steady flows. Adv Water Resour 2005;28(9):964–74.
[33] Tartakovsky AM, Garcia-Naranjo L, Tartakovsky DM. Transient flow in a heterogeneous vadose zone with uncertain parameters. Vadose Zone J 2004;3(1):154–63.
[34] Tartakovsky DM. Probabilistic risk analysis in subsurface hydrology. Geophys Res Lett 2007;34. doi:10.1029/2007GL029245.
[35] Tartakovsky DM, Guadagnini A, Riva M. Stochastic averaging of nonlinear flows in heterogeneous porous media. J Fluid Mech 2003;492:47–62.
[36] Tartakovsky DM, Neuman SP, Lu Z. Conditional stochastic averaging of steady state unsaturated flow by means of Kirchhoff transformation. Water Resour Res 1999;35(3):731–45.
[37] Wang P, Tartakovsky DM. Probabilistic predictions of infiltration into heterogeneous media with uncertain hydraulic parameters. Int J Uncert Quant 2011;1(1):35–47.
[38] Warrick AW. Soil water dynamics. Oxford University Press; 2003.
[39] Winter CL, Tartakovsky DM. Groundwater flow in heterogeneous composite aquifers. Water Resour Res 2002;38(8). doi:10.1029/2001WR00045.
[40] Winter CL, Tartakovsky DM. A reduced complexity model for probabilistic risk assessment of groundwater contamination. Water Resour Res 2008;44:W06501. doi:10.1029/2007WR006599.
[41] Yeh TJ, Gelhar LW, Gutjahr AL. Stochastic analysis of unsaturated flow in heterogeneous soils. 2. Statistically anisotropic media with variable α. Water Resour Res 1985;21(4):457–64.
[42] Zeller KF, Nikolov NT. Quantifying simultaneous fluxes of ozone, carbon dioxide and water vapor above a subalpine forest ecosystem. Environ Pollut 2000;107(1):1–20.
[43] Zhu J, Mohanty BP. Spatial averaging of van Genuchten hydraulic parameters for steady-state flow in heterogeneous soils: a numerical study. Vadose Zone J 2002;1(2):261–72.
[44] Zhu J, Mohanty BP. Soil hydraulic parameter upscaling for steady-state flow with root water uptake. Vadose Zone J 2004;3(4):1464–70.
[45] Zhu J, Young MH, van Genuchten MT. Upscaling schemes and relationships for the Gardner and van Genuchten hydraulic functions for heterogeneous soils. Vadose Zone J 2007;6(1):186–95.